Article:
Ferrer, Alejandro, Tzovenos Starosta, Rodrigo, Ranatunga, Wasantha et al. (2020) Fetal glycosylation defect due to ALG3 and GOG5 variants detected via amniocentesis:complex glycosylation defect with embryonic lethal phenotype. Molecular genetics and metabolism. pp. 424-429. ISSN: 1096-7192

https://doi.org/10.1016/j.ymgme.2020.11.003

Fetal glycosylation defect due to *ALG3* and *GOG5* variants detected via amniocentesis: complex glycosylation defect with embryonic lethal phenotype

Alejandro Ferrer[1],* Rodrigo Tzovenos Starosta[2,3],* Wasantha Ranatunga[2], Dani Ungar[4], Tamas Kozicz[1], Eric Klee[1], Laura M. Rust[2,5], Myra Wick[2,5], Eva Morava[1,2,6]**

1 – Center for Individualized Medicine, Mayo Clinic, Rochester, MN, USA

2 – Department of Clinical Genomics, Mayo Clinic, Rochester, MN, USA

3 – Graduate Program in Genetics and Molecular Biology, Universidade Federal do Rio Grande do Sul, Porto Alegre, RS, Brazil

4 – Department of Biology, University of York, York, UK

5 – Department of Obstetrics and Gynecology, Mayo Clinic, Rochester, MN, USA

6 – Department of Laboratory Medicine and Pathology, Mayo Clinic, Rochester, MN, USA

*Contributed equally to the manuscript

**Corresponding author:

Eva Morava

Mayo Clinic

200 1st St SW

Rochester, MN 55905, USA

Email: morava-kozicz.eva@mayo.edu

AF, TK and EM designed the study. EM obtained funding. LMR and EM conducted the consenting process. AF, RTS, EK, LMR, MJW, and EM reviewed the case. RTS, DU and TK designed the experiments. RTS and WR conducted all experiments. AF and EK performed the bioinformatic analysis. AF and RTS wrote the original draft. WR, DU, TK, EK, LMR, MJW and EM reviewed the draft and made important intellectual contributions. EM obtained funding and coordinated the study. EM made the final decision to submit the manuscript and is the guarantor to this work.

Keywords: congenital disorders of glycosylation; osteochondrodysplasia; fetal cell research; fetal demise; whole-exome sequencing

ABSTRACT

Introduction: Congenital disorders of glycosylation (CDG) are inborn errors of glycan metabolism with high clinical variability. Only a few antenatal cases have been described with CDG. Due to a lack of reliable biomarker, prenatal CDG diagnostics relies primarily on molecular studies. In the presence of variants of uncertain significance prenatal glycosylation studies are very challenging.

Case Report: A consanguineous couple had a history of second-trimester fetal demise with tetralogy of Fallot and skeletal dysplasia. In the consecutive pregnancy, the second trimester ultrasonography showed skeletal dysplasia, vermian hypoplasia, congenital heart defects, omphalocele and dysmorphic features. Prenatal chromosomal microarray revealed a large region of loss of heterozygosity. Demise occurred at 30 weeks. Fetal whole exome sequencing showed a novel homozygous likely pathogenic variant in *ALG3* and a variant of uncertain significance in *COG5*.

Methods: Western blot was used to quantify ALG3, COG5, COG6, and the glycosylation markers ICAM-1 and LAMP2. RT-qPCR was used for *ALG3* and *COG5* expression in cultured amniocytes and compared to age matched controls.

Results: *ALG3* and *COG5* mRNA levels were normal. ICAM-1, LAMP2, ALG3 and COG5 levels were decreased in cultured amniocytes, suggesting the possible involvement of both genes in the complex phenotype.

Conclusion: This is the first case of successful use of glycosylated biomarkers in amniocytes, providing further options of functional antenatal testing in CDG.

INTRODUCTION

Congenital disorders of glycosylation (CDG) are a growing group of rare inherited metabolic disorders that affect the building and processing of glycans. The clinical manifestations of CDG vary depending on the biochemical defect (the impacted glycosylation step) and the molecular background. Due to the extreme rarity of these disorders, for many CDG the full clinical spectrum is not yet known; many of those disorders have a complex, multisystem phenotype including malformations, early-onset metabolic abnormalities, and organ dysfunction. CDG are classified primarily according to the type of glycosylation affected – N-glycosylation (attachment of glycans to the amide group of asparagine residues in proteins) or O-glycosylation (attachment of glycans to the lateral oxygen atom of serine or threonine residues). CDG affecting N-glycosylation are further divided according to whether they affect the assembly of glycans in the endoplasmic reticulum (CDG-I) or the remodeling of those glycans either in the endoplasmic reticulum or the Golgi apparatus (CDG-II). With the implementation of next-generation sequencing (NGS) in clinical practice, the knowledge of the genetic etiology of CDG has expanded enormously with more than 137 different CDG discovered to date (1).

We report a consanguineous couple with two spontaneous pregnancy losses in which the fetuses presented with a similar abnormal phenotype. Whole exome sequencing (WES) of amniocyte DNA obtained from the second miscarriage identified a homozygous missense variant in *COG5* and a homozygous nonsense variant in *ALG3* that were also confirmed by PCR in the first miscarriage. These two genes are included in the N-glycosylation pathway and potentially contributory to fetal demise (2-4). However, both variants were novel and therefore further research testing was pursued.

CASE REPORT

A 28-year-old G6P2122 woman at 12 3/7 weeks gestational age presented for genetic counseling due to a history of previous fetal demise, family history of spinal muscular atrophy, and consanguinity (figure 1A). She and her partner, both of Pakistani ancestry, are the parents of two healthy children, aged 8 and 5 years. The couple also had a pregnancy which resulted in intrauterine fetal demise at 24 4/7 weeks; autopsy revealed tetralogy of Fallot, probable skeletal dysplasia with decreased long bone length (<2nd percentile for gestational age), and dysmorphic findings including micrognathia, slit-like nostrils, and flat upper lip. Chromosomal microarray (CMA) was negative for deletions or duplications, but revealed large regions with loss of heterozygosity (LOH) presumably due to consanguinity (approximately 8%). The patient's obstetrical history also included two first trimester elective terminations.

At 17 weeks gestation of the current pregnancy, early anatomical ultrasound revealed similar anomalies to the prior affected pregnancy (figure 1B) including skeletal dysplasia with shortening of all long bones, short ribs, micrognathia, small nose, vermian hypoplasia, and congenital heart defect. The fetus had the additional finding of an omphalocele and echogenic bowel. Amniocentesis was performed and CMA was negative for deletions and duplications, but revealed 15% LOH.

At 30-1/7 weeks gestational age, the patient experienced preterm onset of labor resulting in delivery of a stillborn infant. The placenta was large-for-gestational-age, friable, and hydropic on pathological examination (figure 1C). WES performed on amniocytes from this second pregnancy identified two homozygous variants of interest (*COG5* c.944C>G, p.Ser315Cys; and *ALG3* c.1188G>A, p.Trp396*) inherited from both healthy, heterozygous carriers parents.

Consequently, placental tissue from the first pregnancy was tested by directed PCR and found to also carry both variants.

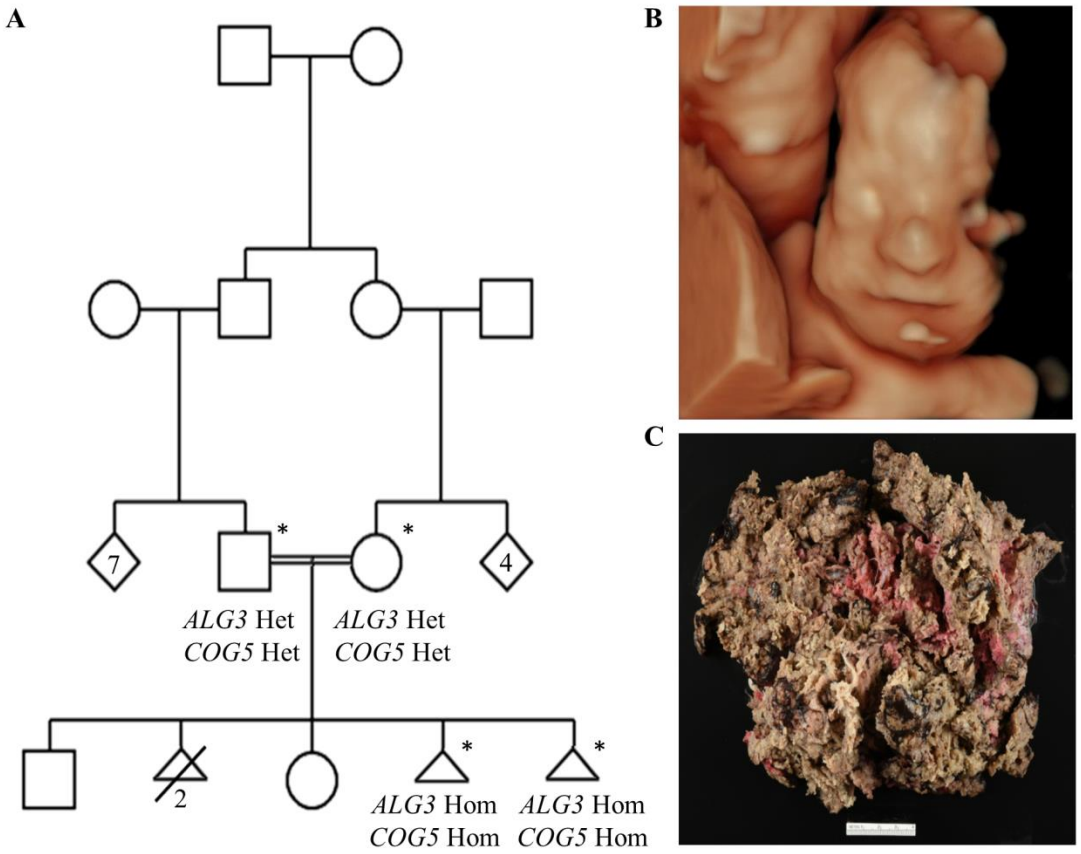

Figure 1: A) Pedigree of the family showing a high degree of consanguinity. Asterisks indicate individuals genetically tested. The genotypes for the variants in *ALG3* and *COG5* are indicated under each symbol. Het: heterozygous, Hom: homozygous. B) Tridimensional reconstruction of fetal ultrasound at gestational age 24 weeks, 6 days showing hypertelorism, depressed nasal bridge, and thin upper lip of the fetus. C) Photograph of the fetal surface of the placenta, showing hydropic, partially disintegrated villi.

METHODS

Whole Exome Sequencing Analysis

WES from the second miscarriage and both parents was performed at the Clinical Genomics Laboratory (Mayo Clinic). Paired-end libraries were prepared using 1.0 µg of genomic DNA using the Agilent Bravo liquid handler (Agilent) as indicated by the manufacturer. Whole exon capture was carried out using 750 ng of the prepped library following the protocol for Agilent's SureSelect Human All Exon v5 + UTRs 75 MB kit. The purified capture products were amplified using the SureSelect Post-Capture Indexing forward and Index PCR reverse primers (Agilent) for 12 cycles. Libraries were sequenced at an average coverage of ~80X following Illumina's standard protocol in an Illumina cBot and HiSeq 3000/4000 PE Cluster Kit. The flow cells were sequenced as 150 X 2 paired end reads on an Illumina HiSeq 4000 using HiSeq 3000/4000 sequencing kit and HCS v3.3.52 collection software. Base-calling is performed using Illumina's RTA version 2.7.3. Data was processed through an in-house bioinformatics pipeline and analyzed using Ingenuity (Qiagen) by the Center for Individualized Medicine (Mayo Clinic).

Variant Segregation Testing

A formalin-fixed, paraffin embedded (FFTE) sample from the placenta of the first miscarriage was used for testing and was used to obtain genomic DNA following a standard clinical procedure. The presence of both the homozygous *COG5* and *ALG3* variants found in the second miscarriage was tested by PCR using the primers described in Table 1 and the Platinum TaqDNA polymerase High Fidelity commercial kit (ThermoFisher Scientist) following the manufacturer indications. The conditions for the melting step were 51˚C (for *COG5*) or 53˚C (for *ALG3*) for 30 s.

Table 1. Primers used for targeted sequencing of *COG5* and *ALG3* variants and mRNA expression levels by RT-PCR .

Gene Symbol	Test	Oligonucleotide Sequence	Orientation	Predicted Size
COG5	Family segregation of c.944C>G variant	5'-CTCAATAAATTATTTCCTAAAGAAGGA-3'	Forward	465 bp
		5'-CAATACTTTTTGTAGATGTTGTACCT-3'	Reverse	
ALG3	Family segregation of c.1188G>A variant	5'-CATACAGATCGTTTCTACCCTCT-3'	Forward	446 bp
		5'-GTGGGCTTTCTTGCTGT-3'	Reverse	
COG5	mRNA expression	5'- TGGGTCCATTCTGTAGACGA-3'	Forward	N/A
		5'- GTTCACTTGCCTGGAAGAGC-3'	Reverse	
ALG3	mRNA expression	5'-CACCTTCTGGGTCATTCACAGG-3'	Forward	N/A
		5'- GTGTCACCCTGCAGTTGGGTATAGT-3'	Reverse	
RNA18S	mRNA expression	5'-GTAACCCGTTGAACCCCATT-3'	Forward	N/A
		5'-CCATCCAATCGGTAGTAGCG-3'	Reverse	
GAPDH	mRNA expression	5'-GCCAAAAGGGTCATCATCTC-3'	Forward	N/A
		5'-GGCCATCCACAGTCTTCT-3'	Reverse	
ACTB	mRNA expression	5'-CATGTACGTTGCTATCCAGGC-3'	Forward	N/A
		5'-CTCCTTAATGTCACGCACGAT-3'	Reverse	

Amniocyte Culture

Amniocytes were obtained from the amniocentesis during the second pregnancy. Primary cultures were established for 9 days before transferring to T25 culture flasks. Cells were incubated at 37°C with 5% CO_2, 5% O_2 and 90% N_2 in 50% Chang C Working Medium (Irvine) and 50% Dulbecco's Modified Eagle Medium Alpha with GlutaMAX (Gibco) supplemented with 12.5% fetal bovine serum (Gibco) and 1% Penicillin/Streptomycin solution (Gibco).

Western blot

Protein extracts from amniocytes were denatured for either 30 minutes at 70ºC (ICAM-1 and LAMP2) or 5 minutes at 95ºC (ALG3, COG5 and COG6) in dithiothreitol (DTT) or β-mercaptoethanol and LDS-containing NuPAGE sample buffer (Novex and Invitrogen, Carlsbad, CA, USA) and loaded into either a 10% (ICAM-1 and ALG3) or a 4-12% (LAMP2, COG5, and COG6) Bis-Tris gel (Invitrogen). Electrophoresis was performed in MOPS SDS NuPAGE

running buffer (Novex) at 200V for 60 minutes, followed by transfer to a nitrocellulose membrane (Bio-Rad laboratories, Germany) in NuPAGE transfer buffer (Novex) at 35V for 180 minutes. Membranes were blocked at either SEA Block blocking buffer (Thermo Scientific, Rockford, IL, USA) (ICAM-1) or 5% blocking-grade non-fat milk (Sigma Aldrich, Saint Louis, MO, USA) or 5% BSA in Tris buffered saline with 0.1% Tween-20 (TBST). Primary antibodies (ICAM-1 mouse monoclonal, Santa Cruz Biotechnology, 1:500; LAMP2 mouse monoclonal, H4B4 clone, Invitrogen, 1:1000; ACTB rabbit monoclonal antibody, ABclonal, 1:10,000; GAPDH mouse monoclonal antibody, Invitrogen, 1:20,000; ALG3 rabbit polyclonal, 1:125, Abnova; COG5 rabbit polyclonal and COG6 rabbit polyclonal provided in house (5), University of York, UK, 1:500) were incubated overnight or 48-72 hours at 4ºC and washed with 0.1% Tween-20 in PBS or TBST (Fisher Bioreagents, Fair Lawn, NJ, USA). For ICAM-1, LAMP2, ALG3, ACTB and GAPDH, a fluorescent-conjugated secondary antibody (donkey anti-mouse cross-adsorbed secondary antibody, DyLight 800 conjugate; donkey anti-rabbit cross-adsorbed secondary antibody, DyLight 680 conjugate; both from Invitrogen) was used. For COG5 and COG6, a biotinylated secondary antibody (Biotin-SP-conjugated AffiniPure donkey anti-rabbit, Jackson ImmunoResearch Laboratories, West Grove, PA, USA, 1:1000) was used. Secondary antibodies were incubated for 1 hour at 4ºC, washed with 0.1% Tween-20 in PBS, and membranes were either detected and quantified in an Odyssey Fc system (Li-Cor Biosciences, Lincoln, NE, USA) or incubated in fluorophore-conjugated streptavidin (AlexaFluor 680-conjugated streptavidin, Jackson ImmunoResearch Laboratories, 1:1000) for 30 min at 4ºC. After incubation with streptavidin, membranes were washed with 0.1% Tween-20 in PBS, detected and quantified in the same Odyssey Fc system.

Real-time quantitative polymerase chain reaction (RT-qPCR)

Isolated RNA from amniocytes was reversed transcribed to cDNA using the SuperScript III First-Strand kit (Invitrogen) according to the manufacturer's protocol (primer sequences were synthesized by Integrated DNA Technologies, Coralville, IA, USA and are available in Table 1). The reverse-transcriptase polymerase chain reaction (RT-PCR) was set up using the following conditions: 65ºC for 5 minutes, 25ºC for 10 minutes, 50ºC for 50 minutes, 85ºC for 5 minutes. For the real-time quantitative polymerase chain reaction (RT-qPCR) mixtures contained each 6.05 µL SYBR Green (Applied Biosystems, Warrington, UK), 3.63 µL double deionized H_2O, 1.21 µL of the respective primers, and 1.1 µL of cDNA. RT-qPCR cycles were performed and read in a LightCycler 480 II (Roche Molecular Systems, Rotkreuz, Switzerland) as follows: pre-incubation at 95ºC for 5 minutes; 45 cycles of amplification at 95ºC for 10 seconds, 60ºC for 10 seconds, 72ºC for 10 seconds; melting curve at 95ºC for 5 seconds and 65ºC for 1 minute; and cooling at 40ºC for 30 seconds.

RESULTS

Genetic Analysis

The analysis of WES data focused on the overlapping LOH areas observed by CMA in both miscarriages, where only three genes (*EDEM3, TMEM140* and *COG5*) were found to carry homozygous rare (below 1% in healthy population (6)) variants. An in-depth review of these results concluded that the variant in *COG5* (c.944C>G; p.Ser315Cys) potentially explained the patient's phenotype. Interestingly, further review identified an additional gene in *N*-glycosylation pathway (*ALG3* – c.1188G>A; p.Trp396*) carrying a homozygous likely pathogenic variant.

The homozygous c.944C>G; p.Ser315Cys variant in *COG5* is a novel variant not reported in the healthy population (gnomAD (6)) or variants databases (ClinVar and HGMD). The amino

acid position is not conserved across species and it is not located in any functional domain described. Some *in silico* predictions suggested a deleterious effect (SIFT, PolyPhen, MutationTaster) although in other cases (M-CAP) was predicted as benign. The constraint values described in gnomAD for this gene indicate tolerance to missense variation. We classified the variant as uncertain significance (VUS) according to ACMG criteria but it was considered relevant due to the possible phenotypic overlap between the two fetuses and other CDG patients including skeletal dysplasia.

On the other hand, the homozygous c.1188G>A; p.Trp396* variant in *ALG3* is classified as likely pathogenic by ACMG criteria but the possible connection with the phenotype observed was not clear. This variant was not present in the healthy population (gnomAD (6)) or variant databases (ClinVar and HGMD). The variant is located in the last exon of the protein and does not impact any functional domain described. It is not predicted to initiate nonsense mediated decay by the 50bp rule but the constraint values described in gnomAD for this gene indicate intolerance to loss of function variations.

Both variants were also detected in the first miscarriage after testing the genomic DNA obtained from a formalin-fixed, paraffin embedded (FFTE) sample by PCR. Unfortunately, healthy siblings were not available for testing.

Glycosylation markers

N-glycosylation markers ICAM1 and LAMP2 analyzed by Western blot were both abnormal in cultured amniocytes from the affected individual compared to cultured amniocyte controls, confirming a glycosylation defect. Decreased abundance of glycosylated ICAM-1 was detected in cultured amniocytes (the protein expression was 61.4% lower than that in control amniocytes),

as shown in figure 2A and B. The LAMP2 protein showed an abnormal migration pattern by Western blot, compatible with abnormal LAMP2 glycosylation in the affected individuals amniocytes compared to controls (figure 2C and D).

Gene expression of *ALG3* and *COG5*

Gene expression studies by RT-qPCR showed no decrease in the level of gene products for either *ALG3* or *COG5* genes, additionally excluding nonsense-mediated decay in the case of *ALG3*. Levels of Cog5 mRNA were similar between affected individual and control amniocytes (figure 2E) while Alg3 mRNA levels were slightly higher in the affected individual's amniocytes (figure 2F).

Protein expression of ALG3, COG5 and COG6

Protein expression of ALG3, COG5 and COG6 (another subunit from the same COG lobe) were all decreased in the affected individual's amniocytes compared to the control amniocytes. The ALG3 Western blot showed two bands corresponding to the two different isoforms of the protein (50kD and 44kD) that were both decreased by 49.8% and 74.3% respectively (Figure 2 G and H). Quantitation of COG5 protein was found 41% lower compared to the control by Western blot, as shown in figure 2J. Similarly, Western blot analysis of COG6 showed a double band (figure 2K and L): the upper band, which is appropriate for the predicted size of 68 kDa for COG6, was 34% decreased in the affected individual's amniocytes compared to controls. The lower band was 30% increased in the affected individual's amniocytes compared to controls (figure 2L). We hypothesize that this band may be the product of proteolytic degradation of COG6.

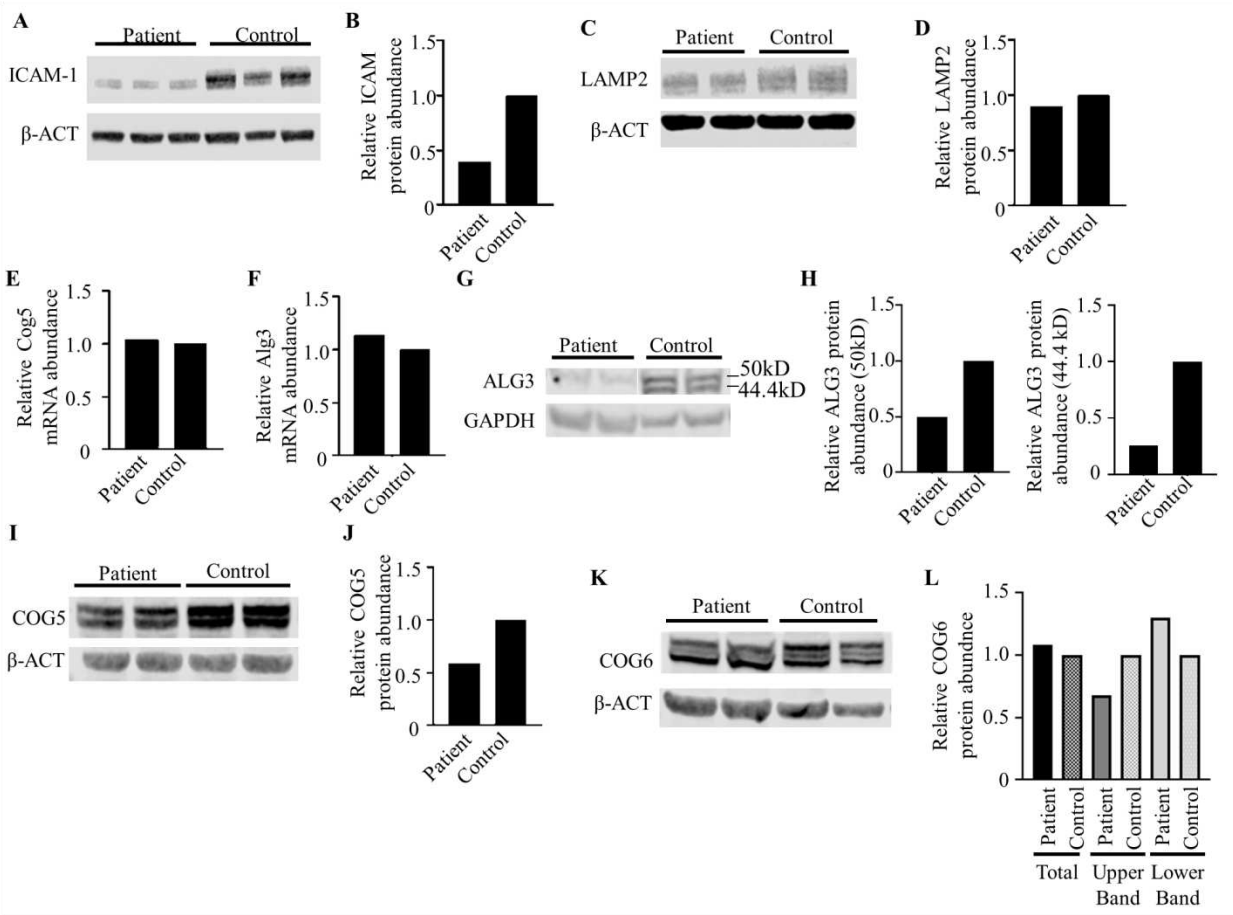

233

234 Figure 2: A) Representative Western blot of patient and control amniocytes against ICAM-1. B)
235 Quantification of Western blot shown in A indicating protein abundance 61.4% lower in the
236 patient, consistent with a glycosylation defect. C) Representative Western blot of patient and
237 control amniocytes against LAMP2. D) Quantification of Western blot shown in C indicating
238 protein abundance 11.4% lower in the patient, as well as an altered protein migration pattern in
239 the patient compared to control, consistent with a glycosylation defect. E) RT-qPCR of Cog5 in
240 patient amniocytes and control amniocytes, averaged against the three housekeeping transcripts
241 Rna18s, Gapdh, and Bact, showing approximately same levels of Cog5 mRNA. F) RT-qPCR of
242 Alg3 in patient amniocytes and control amniocytes, averaged against the three housekeeping
243 transcripts Rna18s, Gapdh, and Bact, showing an increase of 13.3% in mRNA abundance in the

patient. G) Representative Western blot of ALG3 expression in patient amniocytes and control amniocytes. Two bands are present (50kD and 44.4 kD) corresponding to each isoform of ALG3. H) Quantification of Western blot shown in G indicating a protein abundance 49.8% (50kD band) and 74.3% (44.4 kD) lower in the patient compared to control amniocytes. I) Representative Western blot against COG5 in patient amniocytes and control amniocytes. J) Quantification of Western blot shown in I indicating a protein abundance 41% lower in the patient compared to control amniocytes. K) Representative Western blot performed in patient and control amniocytes against COG6. L) Quantification of I showing a lower intensity of the upper band and a higher intensity of the lower band compared to control amniocytes. β-ACT: β-actin; GAPDH: Glyceraldehyde 3-phosphate dehydrogenase.

DISCUSSION

CDG are rare metabolic disorders that affect the assembly and processing of glycans, mainly in the endoplasmic reticulum (ER) and in the Golgi apparatus (7). The CDG group is extremely heterogeneous, ranging from diseases that are tissue-restricted (8) to multi-system organ involvement (9). In most rare CDG our current knowledge of the phenotypic spectrum is biased because it often relies on reports of a single or a few cases. CDG with early fetal loss thus tend to be underdiagnosed and underreported. For example, COG5-CDG, first described as a mild psychomotor delay syndrome (10), was reported in subsequent reports in patients with prenatal features who develop significant complications in multiple systems (11). This high variability also complicates the identification of the genetic cause resulting in the different manifestations of the disease.

Here we report on a consanguineous family with two spontaneous fetal demises showing similar timeframes and phenotype including a heart defect and signs of skeletal dysplasia. WES testing revealed two variants in genes included in the glycosylation pathway (homozygous VUS in *COG5* and homozygous likely pathogenic variants in *ALG3*) inherited from both parents who were both heterozygous carriers. Since both variants were confirmed by PCR to be also present in homozygosis in the first miscarriage, we hypothesized that the phenotype was caused by a glycosylation defect. We evaluated the N-glycosylation pathway in cultured amniocytes obtained from the second pregnancy by measuring two common glycosylation markers using Western blot: ICAM-1 and LAMP2. The expression of both proteins was abnormal compared to control amniocytes (Figure 2A-C). This combined deficit is expected in most CDG, even though decreased abundance of LAMP2 or ICAM-1 in isolation do not always reflect major expression changes in all CDG (12, 13). We performed RT-qPCR studies of gene expression of *COG5* and *ALG3* that indicated normal mRNA levels (Figure 2E and F), suggesting that the presence of the variants did not affect gene expression and a possible alteration would be at the protein level.

The protein levels of ALG3 and COG5 in the affected individual's sample by Western blot were markedly reduced compared to controls (Figure 2G to J). The reduction of ALG3 protein levels could be explained by a higher degradation of the truncated protein as a consequence of the variant, which is supported by the *ALG3* mRNA levels being compared to the controls. In the case of COG5 we postulated that the missense variant could interfere with the formation of lobe B of the COG complex, causing the unassembled protein to be degraded impairing the glycosylation pathway in these individuals. This idea was tested by measuring the presence of COG6 (another COG protein) in the same samples. COG6 was present in two distinct molecular weights (figure 2K and L), with a decrease of the heavier form and an increase in the lighter

289 form. It is possible that this happens due to an increased degradation of COG6 and, being COG6
290 a COG subunit located in the same lobe but not in direct contact with COG5, this suggests the
291 destabilization of the whole lobe B by a mutated COG5. This is in accordance with experiments
292 by Rymen and colleagues showing decreased expression of COG7 (another lobe B subunit) in
293 COG5-CDG (11).

294 With this data we concluded that the probable cause for both fetal losses was a congenital
295 defect of glycosylation. We show evidence that the *ALG3* truncating variant results in decreased
296 protein level, and the *COG5* variant is probably impairing the formation of the COG complex.
297 Therefore, although both defects individually could lead to a CDG phenotype, we cannot rule out
298 an effect in the pathway following a “multiple hit” mechanism of disease impacting the N-
299 glycosylation pathway, starting with the first insult in the ER-related assembly. Although the
300 presence of the protein is not a guarantee for protein function, it is possible that some residual
301 ALG3 activity remains and therefore some glycosylated proteins could be transferred to the
302 Golgi for further processing. There, the additional COG defect would interfere with Golgi
303 trafficking, adding a second biochemical abnormality to already decreased glycosylation. We
304 hypothesize that this could cause truncated glycans similar to a "digenic" mechanism.

305 If this hypothesis is true, we would expect a combined type I/type II glycosylation defect in
306 our patient, similar to that seen in PGM1-CDG. It is interesting to note that our patient had a
307 prenatal presentation of skeletal long bone shortening/short stature, congenital heart
308 malformation and micrognathia, which are also features of PGM1-CDG (14, 15) and have been
309 observed in some of the COG deficiencies, like COG7-CDG (16).

310 In summary, we have provided evidence indicating a glycosylation defect in this family that
311 may have impacted fetal development, leading to fetal demise. Interestingly, it is described that

protein glycosylation plays a major role in development and maintenance in the third trimester of gestation – the period when both miscarriages occurred – also supporting this idea (2-4). Additionally, we show for the first time that studies of glycosylated proteins such as ICAM-1 and LAMP2 can be carried out in cultured amniocytes in the third trimester, leading to the development of more elaborate and elaborate glycoproteomics techniques in pregnancy losses suspected with a diagnosis of CDG (17).

ACKNOWLEDGEMENTS

We want to thank the patient's family for participating in this study and allowing us to publish these results. We also want to thank Kevin Meyer from the Genomics Laboratory at Mayo Clinic for his lab work and assisting with amniocyte culturing. This work was funded by the grant titled Frontiers in Congenital Disorders of Glycosylation (1U54NS115198-01) from the National Institute of Neurological Diseases and Stroke (NINDS) and the National Center for Advancing Translational Sciences (NCATS) and the Rare Disorders Consortium Disease Network (RDCRN) (EM and KR). RTS's participation in this work was funded by Brazil's Programa Institucional de Internacionalização from the Coordenadoria de Aperfeiçoamento de Pessoal de Nível Superior (PRINT/CAPES). DU's participation in this work was part-funded by the Wellcome Trust (ref: 204829) through the Centre for Future Health (CFH) at the University of York.

REFERENCES

1. Ferreira CR, Altassan R, Marques-Da-Silva D, Francisco R, Jaeken J, Morava E. Recognizable phenotypes in CDG. J Inherit Metab Dis. 2018;41(3):541-53.

2. Altassan R, Peanne R, Jaeken J, Barone R, Bidet M, Borgel D, et al. International clinical guidelines for the management of phosphomannomutase 2-congenital disorders of glycosylation: Diagnosis, treatment and follow up. J Inherit Metab Dis. 2019;42(1):5-28.
3. Fisher P, Ungar D. Bridging the Gap between Glycosylation and Vesicle Traffic. Front Cell Dev Biol. 2016;4:15.
4. Ioffe E, Stanley P. Mice lacking N-acetylglucosaminyltransferase I activity die at mid-gestation, revealing an essential role for complex or hybrid N-linked carbohydrates. Proc Natl Acad Sci U S A. 1994;91(2):728-32.
5. Ungar D, Oka T, Brittle EE, Vasile E, Lupashin VV, Chatterton JE, et al. Characterization of a mammalian Golgi-localized protein complex, COG, that is required for normal Golgi morphology and function. J Cell Biol. 2002;157(3):405-15.
6. Karczewski KJ, Francioli LC, Tiao G, Cummings BB, Alföldi J, Wang Q, et al. Variation across 141,456 human exomes and genomes reveals the spectrum of loss-of-function intolerance across human protein-coding genes. bioRxiv. 2019.
7. Sparks SE, Krasnewich DM. Congenital Disorders of N-Linked Glycosylation and Multiple Pathway Overview. In: Adam MP, Ardinger HH, Pagon RA, Wallace SE, Bean LJH, Stephens K, et al., editors. GeneReviews((R)). Seattle (WA)1993.
8. Lam BL, Zuchner SL, Dallman J, Wen R, Alfonso EC, Vance JM, et al. Mutation K42E in dehydrodolichol diphosphate synthase (DHDDS) causes recessive retinitis pigmentosa. Adv Exp Med Biol. 2014;801:165-70.
9. Verheijen J, Tahata S, Kozicz T, Witters P, Morava E. Therapeutic approaches in Congenital Disorders of Glycosylation (CDG) involving N-linked glycosylation: an update. Genet Med. 2020;22(2):268-79.
10. Paesold-Burda P, Maag C, Troxler H, Foulquier F, Kleinert P, Schnabel S, et al. Deficiency in COG5 causes a moderate form of congenital disorders of glycosylation. Hum Mol Genet. 2009;18(22):4350-6.
11. Rymen D, Keldermans L, Race V, Regal L, Deconinck N, Dionisi-Vici C, et al. COG5-CDG: expanding the clinical spectrum. Orphanet J Rare Dis. 2012;7:94.
12. Radenkovic S, Bird MJ, Emmerzaal TL, Wong SY, Felgueira C, Stiers KM, et al. The Metabolic Map into the Pathomechanism and Treatment of PGM1-CDG. Am J Hum Genet. 2019;104(5):835-46.
13. He P, Srikrishna G, Freeze HH. N-glycosylation deficiency reduces ICAM-1 induction and impairs inflammatory response. Glycobiology. 2014;24(4):392-8.
14. Altassan R, Radenkovic S, Edmondson AC, Barone R, Brasil S, Cechova A, et al. International consensus guidelines for phosphoglucomutase 1 deficiency (PGM1-CDG): Diagnosis, follow-up, and management. J Inherit Metab Dis. 2020.
15. Wong SY, Beamer LJ, Gadomski T, Honzik T, Mohamed M, Wortmann SB, et al. Defining the Phenotype and Assessing Severity in Phosphoglucomutase-1 Deficiency. J Pediatr. 2016;175:130-6 e8.
16. Medrano C, Vega A, Navarrete R, Ecay MJ, Calvo R, Pascual SI, et al. Clinical and molecular diagnosis of non-phosphomannomutase 2 N-linked congenital disorders of glycosylation in Spain. Clin Genet. 2019;95(5):615-26.
17. Abu Bakar N, Lefeber DJ, van Scherpenzeel M. Clinical glycomics for the diagnosis of congenital disorders of glycosylation. J Inherit Metab Dis. 2018;41(3):499-513.